

Review

# Application of Highly Immunocompromised Mice for the Establishment of Patient-Derived Xenograft (PDX) Models

Seiji Okada <sup>1,2,\*</sup> , Kulthida Vaeteewoottacharn <sup>1,3,4</sup> and Ryusho Kariya <sup>1</sup>

<sup>1</sup> Division of Hematopoiesis, Joint Research Center for Human Retrovirus Infection, Kumamoto University, Kumamoto 860-0811, Japan

<sup>2</sup> Graduate School of Medical Sciences, Kumamoto University, Kumamoto 860-0811, Japan

<sup>3</sup> Department of Biochemistry, Khon Kaen University, Khon Kaen 40002, Thailand

<sup>4</sup> Cholangiocarcinoma Research Institute, Khon Kaen University, Khon Kaen 40002, Thailand

\* Correspondence: okadas@kumamoto-u.ac.jp; Tel.: +81-9-6373-6522

Received: 20 June 2019; Accepted: 9 August 2019; Published: 13 August 2019



**Abstract:** Patient-derived xenograft (PDX) models are created by engraftment of patient tumor tissues into immunocompetent mice. Since a PDX model retains the characteristics of the primary patient tumor including gene expression profiles and drug responses, it has become the most reliable in vivo human cancer model. The engraftment rate increases with the introduction of Non-obese diabetic Severe combined immunodeficiency (NOD/SCID)-based immunocompromised mice, especially the NK-deficient NOD strains NOD/SCID/interleukin-2 receptor gamma chain(IL2R $\gamma$ )<sup>null</sup> (NOG/NSG) and NOD/SCID/Jak3(Janus kinase 3)<sup>null</sup> (NOJ). Success rates differ with tumor origin: gastrointestinal tumors acquire a higher engraftment rate, while the rate is lower for breast cancers. Subcutaneous transplantation is the most popular method to establish PDX, but some tumors require specific environments, e.g., orthotopic or renal capsule transplantation. Human hormone treatment is necessary to establish hormone-dependent cancers such as prostate and breast cancers. PDX mice with human hematopoietic and immune systems (humanized PDX) are powerful tools for the analysis of tumor-immune system interaction and evaluation of immunotherapy response. A PDX biobank equipped with patients' clinical data, gene-expression patterns, mutational statuses, tumor tissue architects, and drug responsiveness will be an authoritative resource for developing specific tumor biomarkers for chemotherapeutic predictions, creating individualized therapy, and establishing precise cancer medicine.

**Keywords:** patient-derived xenograft; immunocompromised mice; precision medicine; drug screening; cancer; cell line; cancer immunotherapy; humanized mice

## 1. Introduction

Preclinical studies using animal models are essential for drug development. Fewer than 10% of candidate drugs are approved for the market, even if preclinical trials are successful [1]. This figure is lower for oncology drugs, at approximately 5% [2]. One possible reason is the lack of appropriate human cancer models. Mouse tumors and human-cell-line-transplanted animal models are not always representative of human cancer pathologies, contributing to distinct drug responses [3]. Mice and humans are considerably different [4], and human cancer cell lines somehow lose their original tumor characteristics when transplanted [5]. Accordingly, the National Cancer Institute (NCI, MD, USA) recently decided to replace the NCI-60, a panel of 60 human cell lines, with patient-derived xenografts (PDXs) for drug screening [3]. The PDXs are established by direct engraftment of a patient tumor into an immunocompromised mouse, maintaining the tumor growth in vivo. This has become an essential

tool for preclinical and translational research, particularly for investigations of tumor pathology and for chemotherapeutic drug development. With the introduction of highly immunocompromised mice as recipients, PDX use is now widespread and is becoming a standard “Avatar” model for human cancer research.

## 2. Establishment of Immunocompromised Mice

### 2.1. Nude Mice

In 1962, the first known immunocompromised mice were discovered by Grist (Ruchill Hospital, Glasgow, UK). The “nude” nickname was given because they lacked body fur. Flanagan [6] showed that nude mice also lacked thymus and T lymphocytes; as a result, the adaptive immune responses, including T cell-mediated immune responses and antibody formation that require helper T cells, are defective in nude mice. Since then, nude mice have been used as recipients for human tumor xenografts. However, the intact (or rather activated) innate immunity in nude mice limits the options for human cancer transplantation [7]. In addition, nude mice show leakage of T cells with age [8].

### 2.2. Severe Combined Immunodeficient Mice

In 1983, Bosma [9] (Fox Chase Cancer Institute, PA, USA) first described the severe combined immunodeficient (SCID) mice that lack both functional T and B lymphocytes. The maturation deficiencies of B and T lymphocytes in SCID mice are due to the deletion of *Prkdc* (protein kinase, DNA activated, catalytic polypeptide: DNA-PKCs) and the absence of variable (V)-diversity (D)-joining (J) recombination (V(D)J recombination). The SCID mice were first used as recipients of human hematopoietic stem cells (HSCs) and peripheral blood mononuclear cell (PBMC) transplantation [10,11]. The engraftment efficiency of human tumors is higher in SCID mice compared to nude mice [12]. However, the transplantation efficiencies of human blood cells and tumor cells are not as high as expected, as the remnant natural killer (NK) cells prevent homing and maintenance of human cells. To overcome the effects of NK cells, SCID/Beige mice were established by crossbreeding SCID mice and Beige mice [13]. In addition to the T and B deficiency of SCID mice, the SCID/Beige mice displayed severely reduced NK cell functioning along with the phagocytosis of Beige mice [14]. The uptake rate of human tumor cells increased in SCID/Beige mice compared with SCID mice, as expected [14], but the engraftment rate of human HSCs was not noticeably increased [15].

### 2.3. Non-Obese Diabetic/SCID Mice and NOD/SCID-Based Immunocompromised Mice

Non-obese diabetic (NOD) mice, discovered in 1980 by Makino (Shionogi Co. Osaka, Japan), have diabetes mellitus caused by infiltration of and pancreatic islet destruction by T lymphocytes [16]. Later, it was discovered that NOD mice acquire multiple immune abnormalities including loss of complement and impaired NK, macrophage, and dendritic cell functions [17]. The NOD/SCID mice were established by crossbreeding NOD and SCID mice. The NOD/SCID mice do not develop diabetes because they lose functional T lymphocytes. Moreover, multiple defects in innate and adaptive immunity are seen in these mice, making them better recipients for human hematopoietic stem cell and human solid tumor transplantation [18]. However, there are some residual NK activities in NOD/SCID mice, and several attempts were made to eliminate or suppress these and to improve transplantation efficiency. These attempts included the use of anti-interleukin (IL)-2 receptor antibody or anti-ganglio-N-tetraosylceramide (asialoGM1) antibody and crossbreeding with  $\beta$ 2 macroglobulin- or perforin-deficient mice. The common  $\gamma$  chain ( $\gamma$ c, CD132), also known as IL-2 receptor subunit gamma (IL2R $\gamma$ ), is a cytokine receptor sub-unit. It is common to the receptor complexes for six different interleukin receptors, IL-2, IL-4, IL-7, IL-9, IL-15, and IL-21, which are critical for lymphocyte and NK cell development [19]. The IL2R $\gamma$  interacts with the Janus kinase 3 (Jak3) non-receptor-type tyrosine kinase for signal transduction. Therefore, IL2R $\gamma$ - and Jak3-deficient mice show common phenotypes such as NK deficiency and reduction of T and B lymphocytes [20]. Thus, NOD/SCID mice with complete loss of

NK cells were established by crossbreeding with IL-2 receptor  $\gamma$ -deficient mice (NOD/SCID/IL2R $\gamma^{\text{null}}$ : NOG [21], NOD/SCID/IL2R $\gamma^{\text{null}}$ : NSG [22]) or Jak3-deficient mice (NOD/SCID/Jak3 $^{\text{null}}$ : NOJ [23]) (Table 1). NOG mice have a NOD/ShiJic-Prkdc $^{\text{scid}}$  background with partial deficiency of IL2R $\gamma$  [21], whereas NSG mice have a NOD/ShiSzJ-Prkdc $^{\text{scid}}$  background with complete deficiency of IL2R $\gamma$  [10]. The NSG mice acquire higher engraftment capacity of cord-blood-derived CD34 $^{+}$  cells [24] and higher body weights [25], but these differences do not appear to affect the PDX transplantation efficiency [25]. Moreover, signal regulatory protein alpha (Sirp $\alpha$ ) polymorphism in NOD strains provides superior opportunities for human cell engraftment because SIRP $\alpha$  interacts with human CD47 [26] and suppresses macrophage-mediated phagocytosis, or contributes to the so-called “don’t eat me” signal (Figure 1) [27,28].

**Table 1.** NOD/SCID-based immunocompromised mice.

Mice	NOD/SCID	NOG	NSG	NOJ
Strain	NOD.Cg-Prkdc $^{\text{scid}}$	NOD.Cg-Prkdc $^{\text{scid}}$ Il2rg $^{\text{tm1Sug}}/Jic$	NOD.Cg-Prkdc $^{\text{scid}}$ Il2rg $^{\text{tm1Wjl}}/SzJ$	NOD.Cg-Prkdc $^{\text{scid}}$ Jak3 $^{\text{tm1Card}}$
Genetic defects	SCID	SCID, IL-2 $\gamma$ Partial deficiency	SCID, IL-2 $\gamma$ Complete deficiency	SCID, Jak3 deficiency
Developer	CIEA <sup>1</sup> , Jackson Laboratory	CIEA <sup>1</sup>	Jackson Laboratory	Kumamoto University
Supplier	Japan Clea Charles River	Japan Clea	Charles River	Kumamoto University
NK activities	NK cell dysfunction	Complete loss of NK cells	Complete loss of NK cells	Complete loss of NK cells
Reference	[18]	[21]	[22]	[23]

<sup>1</sup> Central Institute for Experimental Animals (CIEA). NOD = non-obese diabetic; SCID = severe combined immunodeficient; NOG = NOD/SCID/IL-2 receptor  $\gamma$ -deficient (IL2R $\gamma^{\text{null}}$ ); NSG = NOD/SCID/IL2R $\gamma^{\text{null}}$ ; NOJ = NOD/SCID/Janus kinase 3 deficient (Jak3); Prkdc = protein kinase, DNA activated, catalytic polypeptide; NK = natural killer.

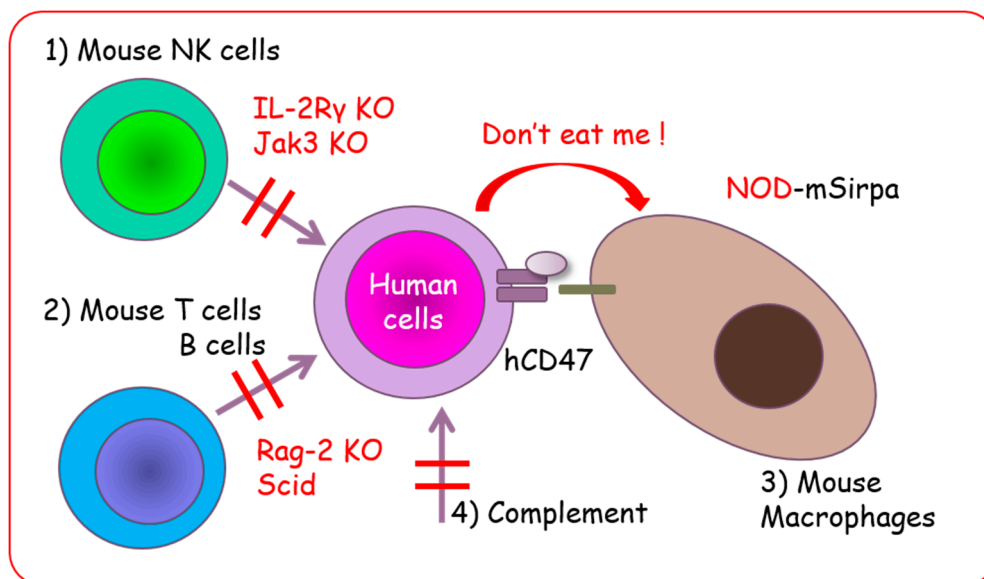


**Figure 1.** NOG, NSG, and NOJ mice with multiple immune deficiencies are excellent recipients for human cell engraftment. (1) Loss of NK cells; (2) loss of acquired immunity by T and B lymphocyte deficiency; (3) “Don’t eat me” signal by NOD-signal regulatory protein alpha (Sirp $\alpha$ ); and (4) loss of complement.

#### 2.4. BALB/c Background Immunocompromised Mice

The BALB/c mice also have Sirp $\alpha$  polymorphisms that acquire binding affinity to human CD47. Hence, BALB/c strain immunocompromised mice, such as BALB/c Rag-2 $^{\text{null}}$ /IL2R $\gamma^{\text{null}}$  (BRG) [29] and Rag-2 $^{\text{null}}$ /Jak3 $^{\text{null}}$  (BRJ) mice [30] have lower macrophage-mediated phagocytosis of human cells, and might be useful recipients for human cell and tissue transplantations [31,32]. Other mice such as C57/BL6 have lower affinity for engrafting human normal and malignant cells [30,33]. Even though the mutations in SCID mice are useful for T and B cell elimination, there are several disadvantages to SCID

mice, such as high susceptibility to irradiation or drugs, and leakage of T lymphocytes. (Recombination activating gene-1/2 (Rag-1/Rag-2) knockout mice are generated to 1) solve these problems and 2) eliminate mature lymphocytes (Table 2) [29,34]. The BRG mice with human Sirp $\alpha$  (SRG) were also generated to improve the engraftment efficiency of PDX (Figure 1) [35].

**Table 2.** Comparison of SCID and Rag-1/Rag-2 mutation.

Mice	SCID	Rag-1/Rag-2 Knock Out Mice
Chromosome	Chr.16	Chr.11 p13
Mutated gene	<i>Prkdc</i>	Recombination-activation gene-1/-2
Mutation	Natural mutant	Homologous recombination
Immunological phenotype	Deficiency of mature B and T lymphocytes NK cells are normal	Deficiency of mature B and T lymphocytes NK cells were normal
Radiation sensitivity	Sensitive (Lethal dose < 3 Gy)	Normal (Lethal dose 9 Gy)
Leakiness	Leaky	None

Rag = recombination activating gene.

### 3. Establishment and Application of Nude/Hairless Immunocompromised Mice

Although more combined immunocompromised mice have been developed, nude mice remained valuable for human tumor engraftment due to the fact of their advantages for tumor monitoring. Tumor visualization by direct observation and imaging in nude mice provides an excellent opportunity for tumor observation in vivo. For this reason, BALB/c Nude Rag-2/Jak3 double-deficient (Nude R/J) mice were established in our lab by mating nude mice with Rag-2<sup>null</sup> and Jak3<sup>null</sup> mice with a BALB/c background [36,37]. Nude R/J mice have no B and T lymphocytes with Rag-2 deficiency, no NK cells with Jak3 deficiency, and have the “don’t eat me signal” with a BALB/c background. Nude R/J mice retained the advantages of no fur and a higher immunocompromisation level than Nude mice, and were, consequently, optimal for in vivo imaging (Figure 2). Another type of furless mouse, namely, the hairless mouse, is also available. Hairless mice have no noticeable immunocompromised phenotypes [38,39]. The SCID Hairless (SHO) mice (Charles River, MA, USA) and Hairless NOD/SCID mice (Envigo, Huntingdon, UK) were established by crossbreeding with hairless mice and used for in vivo imaging (Table 3) [40,41]; however, the engraftment efficiencies were lower than for NK-deficient strains [42]. Mice expressing fluorescence proteins are a powerful tool in cancer research, particularly for visualization of the tumor–host interaction [43]. Several fluorescence-expressing immunocompromised mice have been established and utilized (Figure 3) [44–47]. The relationships between human tumors and the host microenvironment, including vessels, tumor-associated macrophages (TAMs), and cancer-associated fibroblasts (CAFs), can potentially be studied using these models [48].

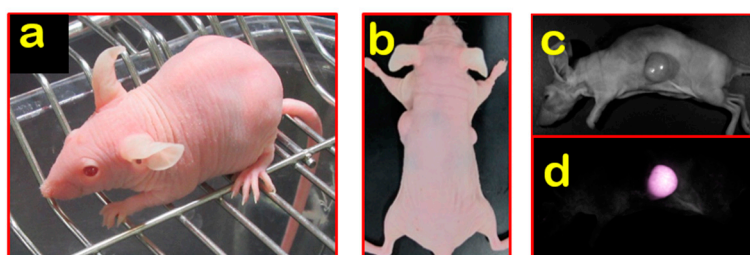


**Figure 2.** Nude R/J mice: (a) BALB/c Nude Rag-2/Jak3 double-deficient (Nude R/J) hairless phenotype; (b) direct visualization of subcutaneous tumor nodules in Nude R/J; (c–d) fluorescent signals observed in Nude R/J.

**Table 3.** Comparison of hairless mice.

Mice	Hairless	Nude	SCID Hairless	Nude R/J
Strain	BALB/c	BALB/c	CB17.Cg/ICR	BALB/c
Gene abnormality	Hairless	<i>Foxn1</i>	Hairless, SCID	<i>Foxn1</i> , Rag-2, Jak3
Immune system	T cells	+	–	–
	B cells	+	–	–
	NK cells	+	+	–
Hair coat	None	None	None	None

+: intact certain immune cells, –: lack of certain cells. Foxn1 = forkhead box N1.

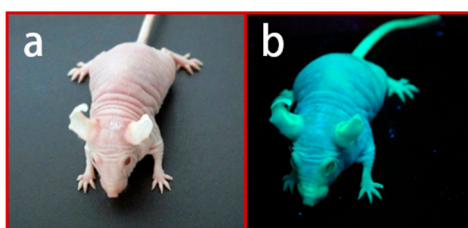


**Figure 3.** Green fluorescence protein (GFP)-expressing Nude R/J mice: (a) GFP Nude R/J phenotype; (b) strong GFP expression under  $\beta$ -actin promoter yields a very bright green signal under UV light [46].

#### 4. Establishment of PDX Models Using Various Immunocompromised Mice

The PDX models were generated by direct transplantation of patient tumor samples into immunocompromised mice (Figure 4). A significant advantage of PDX models is that they retain key characteristics of the patient’s tumor, such as the gene expression profile and heterogeneity of tumor cells [49–51]. Currently, PDX models are the most clinically relevant in vivo cancer models and the most concordant drug response model to human cancer [31,49,52–56]. Thus, the US National Cancer Institute (NCI) decided to substitute a panel of 60 human cell lines (NCI-60) with PDX models for drug screening [3].

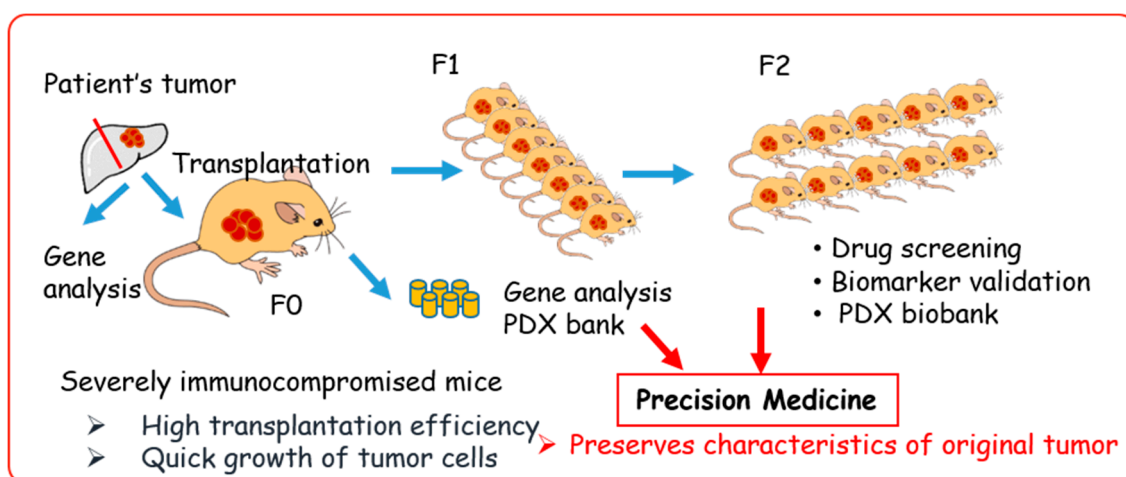


**Figure 4.** Patient-derived xenograft (PDX) model in precision medicine.

The duration of tumor establishment in mice differs among tumors, taking from a few days to a few months for the tumor nodule to be observed (first generation; F0). After serial transplantation, the duration of tumor growth becomes stable, with approximately 40–50 days required to obtain certain sized tumors [53,57]. The PDX samples should be stored together with the patient’s clinical data, gene-expression patterns, mutational statuses, drug responsiveness, and pathological analysis to generate a PDX library.



Nude mice have been used to generate PDX models with reasonable efficacy and are used as a standard recipient (Table 4). With this model, the engraftment efficiencies of gastrointestinal tumors are relatively high, while the establishment of hematological malignancy PDXs are almost impossible in nude mice. The introduction of SCID and NOD/SCID mice increased PDX success rates [58]. As NOD/SCID mice have relatively short lifespans and spontaneously develop thymic lymphoma [18], more immunocompromised mice, such as NOG/NSG mice [59–61], are a more appropriate model. The NOG/NSG mice are the most immunocompromised mice available and show the highest engraftment efficiencies for both normal and malignant human tissues [53]. However, NOG/NSG mice must be kept under especially clean specific pathogen-free (SPF) conditions; hence, culture prices are relatively high (100 US\$ per mouse for academic use in Japan). Moreover, breeding of these mice is not possible by the users. Since nude mice have benefits such as a relatively high engraftment ratios of gastrointestinal tumors, easy observation of subcutaneous tumors, and relatively low price, they remain an important resource for PDX establishment [31,53,62]. The BRJ mice have been used as alternative recipients of cholangiocarcinoma PDX, with a high engraftment ratio (75%) [57,63]. Other solid tumors, such as head and neck tumors, gastric cancers, and bladder cancers, are now under investigation. From our preliminary study, BRJ successfully acquired human solid cancers with relatively high engraftment ratios (compared to currently available models, data not shown) (Figure 5). Since BRJ mice are easy to breed and maintain by users, they are good candidates for PDX, and since Nude R/J mice have the benefits of both BRJ and nude mice, they may be the ideal model for passaging and drug evaluation [36].

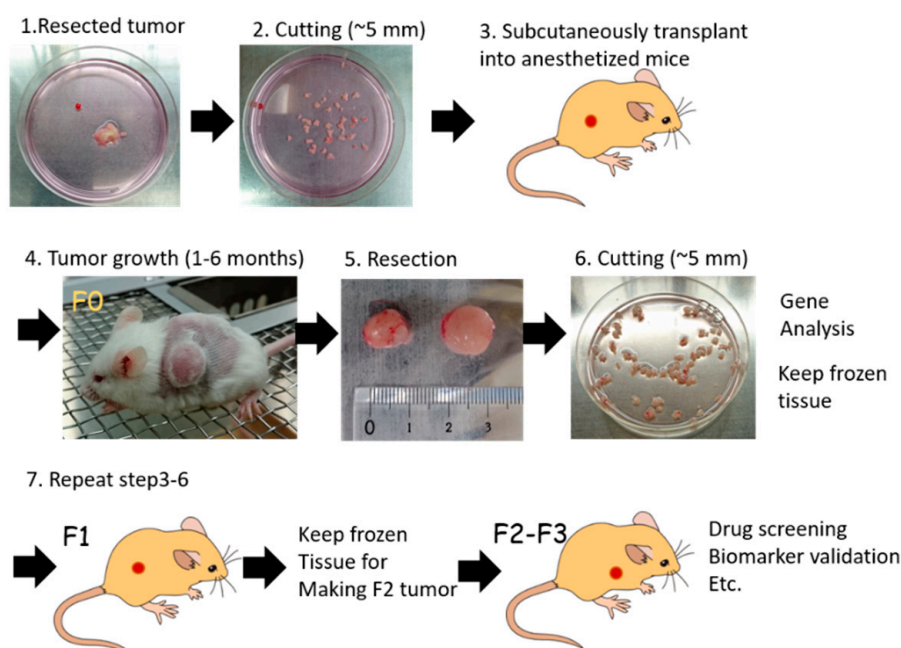


**Figure 5.** Generation process of PDX. Surgical specimen from a patient’s tumor (1) is divided into small pieces (2) and transplanted into an anesthetized immunocompromised mouse (3). Tumor growth takes 1 to 6 months (4). Once tumors are grown in F0 mice, xenografts are resected (5) and cut into small pieces (6). Parts of tumor tissues are analyzed for tumor characteristics, such as whole exome sequencing (WES), RNA sequencing (RNA-seq), and copy number variation (CNV) analysis. The remnant PDX tumor is stored in liquid nitrogen, or further transplanted into immunocompetent mice (7) for expansion. Conventionally, F2 or F3 PDX tumors are used for cancer biology study, such as drug sensitivity screening, identifying biomarkers, etc.

**Table 4.** Immunocompromised mouse strains for PDX.

Mouse Strain	Phenotype	Advantage	Disadvantage/Consideration	Success Rate of PDX
Nude	No thymus, no coat of hair	Well characterized, easy to detect s.c. tumor	Functional B and NK cells, increased T cell leakage with age	Low
SCID	No mature T and B cells	Better engraftment compared with nude	Functional NK cell, leakage of T cells, radiosensitive	Low
SCID/Beige	No mature T and B cells, impaired M $\phi$ and NK function	Better engraftment compared with SCID	Leakage of T cells, radiosensitive	Moderate
NOD/SCID	No mature T and B cells Impaired NK function Impaired M $\phi$ & DC	Better engraftment	Spontaneous lymphoma Short life span (av. 36wks) Radiosensitive	Moderate
NOG/NSG/NOJ	No mature T and B cells, no NK cells, impaired M $\phi$ and DC	Excellent engraftment of PDX including hematopoietic malignancies	Need strict SPF conditions, breeding is not easy, expensive	High
BALB/c Rag2 <sup>null</sup> /IL2R $\gamma$ <sup>null</sup> (BRG) Rag-2 <sup>null</sup> /Jak3 <sup>null</sup> (BRJ)	No mature T and B cells, no NK cells	Excellent engraftment of PDX, resistant to stress, easy breeding, radio resistant		High

NK: natural killer cells, M $\phi$ : macrophages, DCs: dendritic cells, NOG/NSG: NOD/SCID/IL2R $\gamma$ <sup>null</sup>, NOJ: NOD/SCID/Jak3<sup>null</sup>, s.c.: subcutaneous.

Success rates of PDX establishment vary by tumor origin and disease characteristics such as tumor aggressiveness, relapse/recurrence status, and primary or metastatic tumor. More aggressive, relapsed and highly metastatic tumors tend to show higher transplantation rates [53]. Gastrointestinal cancers, such as colon and pancreatic cancers, seem to have higher engraftment ratios compared with other cancers. Engraftment ratios are also higher in more immunocompromised mice (Nude < SCID < NOD/SCID < NSG) (Table 5) [53]. The engraftment ratio for breast cancer is relatively low, and orthotopic transplantation is needed [64]. Orthotopic and renal capsule engraftment clearly increase the engraftment ratio for some tumors, although special techniques are required [31,65,66]. For hematological malignancies such as leukemia and multiple myeloma, direct engraftment into the bloodstream or into the bone marrow of NOG/NSG mice is necessary. Human hormone replacement supports hormone-dependent tumors such as breast and prostate cancers [67–69].

## 5. Generation of PDX-Derived Cell Lines

A tumor cell line can be generated from a PDX tissue sample [57,70,71]. The establishment of tumor cell lines from primary tissues is relatively difficult with the conventional protocol because fibroblasts often outgrow and overcome the cancer cell growth in vitro. In PDX tissue, human fibroblasts are substituted by murine fibroblasts. These mouse fibroblasts have shorter lifespans and are more sensitive to mechanical and enzymatic removal, so the elimination of fibroblasts takes less time. As mentioned earlier, fluorescence-emitting immunocompromised mice have also been developed. These mice have superior benefits for distinguishing engrafted tumor cells and mouse-derived cells [46,72] and, thus, may be useful for establishing PDX-derived cancer cell lines. These PDX-derived tumor cell lines are useful for high-throughput drug screening, as they retain the characteristics of the primary tumors. It is worth mentioning that, in some cases, male-derived tumor tissues retain the Y chromosome in PDX but lose it during cell line development. This might imply that at least one more mutation is required to establish PDX-derived cell lines [57].

## 6. PDX in Humanized Mice

The immune system plays an essential role in tumor control. Recently, cancer immunotherapy using various approaches including antibodies, cancer vaccines, adoptive cell therapies, and immune checkpoint blockade therapies has gained attention as a promising and effective modality with fewer side effects [73–75]. However, a mouse model that allows monitoring of the immune response is needed to test these newly developed therapies, because the current PDX model lacks principal immune cells. Mice with a reconstituted human immune system, so-called humanized mice, are available. Humanized mice are generated by transplantation of human hematopoietic stem cells into highly immunocompromised mice such as NOG, NSG, and NOJ [21–23,76]. Originally used for pathological studies of human-specific pathogens, these models can mimic the human immune system to a certain degree, but they do not represent a complete and functional human immune system. The mouse bone marrow and thymic microenvironments are different from humans and, therefore, the T cells are not fully developed. Moreover, myeloid and erythroid cell development in these mice are lower than in humans. The humanized bone marrow–liver–thymus (BLT) mouse model can be generated by engraftment of human fetal liver and thymus along with human hematopoietic stem cells into an immunocompromised mouse renal capsule [77]. Since the BLT mouse harbors a nearly complete human immune system including functional T cell response, it is a powerful tool to study human immunology and immunotherapy. However, BLT usage is greatly limited by ethical issues including a restricted supply of the human fetal thymus and liver tissues needed to generate these mice. Human leukocyte antigen (HLA) class I and class II transgenic mice, and several types of NOG/NSG mice with human cytokine transgenes, have been developed to overcome some of these limitations [78,79] (Figure 6). The NSG mice that express human stem cell factor, granulocyte-macrophage colony stimulating factor, and interleukin-3, termed NSG-SGM3, showed robust human hematopoietic reconstitution, a higher frequency of human myeloid cells, and increased regulatory T-cell development [80]. The HLA-expressing humanized mice



develop functional HLA-restricted T cells [81,82]. Attempts have also been made to introduce the human hematopoietic microenvironment into immunocompromised mice [83]. These mice represent a very useful model to reconstitute a more accurate human immune system against human malignancies.

**Table 5.** PDX success rates in different immunocompromised mice.

Tumor Type	Mice Strain	Implantation Site	Number of Sample	Engraftment Ratio	References
Cholangiocarcinoma	SCID	s.c. *	55	34.5%	Ojima, 2010 [84]
	NOD/SCID	s.c.	20	5.8%	Cavalloni, 2016 [85]
	BRJ	s.c.	16	75%	Vaeteewoottacharn, 2019 [57]
Colorectal cancer	Nude	s.c.	85	63.5%	Julien, 2012 [86]
	NOD/SCID	s.c.	85	87%	Bertolini, 2011 [87]
	NSG	s.c.	27	54%	Chou, 2013 [88]
Pancreatic cancer	Nude	s.c.	69	61%	Garrido-Laguna, 2011 [89]
	SCID	s.c.	12	67%	Mattie, 2013 [90]
	NSG	s.c.	121	71.1%	Guo, 2019 [91]
Gastric cancer	Nude	s.c.	32	73.7%	Wang, 2017 [92]
	NOD/SCID	s.c.	185	34.1%	Zhu, 2015 [93]
	Nude/SCID	s.c.	83/119	16.9%/26.9%	Zhang, 2015 [94]
	Nude/NOG	s.c.	62	24.2%	Choi, 2016 [95]
Head and neck cancer	Nude	s.c.	46	54%	Keysar, 2013 [96]
	NSG	s.c.	26	84.6%	Kimple, 2013 [97]
Breast cancer	Nude	s.c.	200	12.5%	Marangoni, 2007 [98]
	Nude	fat pad **	314	2.5% (ER+)	Cottu, 2012 [99]
	Nude	fat pad	109	24.3% (ER−)	
	NOD/SCID	fat pad	49	27%	DeRose, 2011 [100]
	SCID/Beige	s.c.	162	19%	Zhang, 2013 [101]
Ovarian cancer	NSG	s.c.	32	31.3%	
	Nude	s.c.	138	25%	Ricci, 2014 [102]
	Nude	r.c. ***	45	48.8%	Heo, 2017 [103]
	SCID	s.c.	34	50%	Dobbin, 2014 [104]
	SCID	s.c.	168	74%	Weroha, 2014 [105]
Non-small lung cancer	NSG	s.c.	12	83%	Topp, 2014 [106]
	NOD/SCID	s.c.	102	25%	Fichtner, 2008 [107]
	NOD/SCID	r.c.	527	90%	Dong, 2010 [108]
	NOD/SCID	s.c.	308	26%	Chen, 2019 [109]
Glioblastoma	NSG	s.c.	441	28.7%	Wang, 2017 [51]
	NSG	orthotopic	100	30%	Brabetz, 2018 [110]
	Nude	s.c.	23	39%	Priolo, 2010 [111]
	NOD/SCID	s.c.	23	48%	
Prostate	SCID	s.c.	86	58.1%	Wang, 2005 [66]
	SCID	orthotopic	57	71.9%	
	SCID	r.c.	122	93.4%	
	NSG	s.c.	27	37%	Wetterauer, 2015 [112]
	Renal cell carcinoma	Nude	s.c.	336	8.9%
NOD/SCID		r.c.	94	37.2%	Sivanand, 2013 [114]
NSG		s.c.	74	45%	Dong, 2017 [115]
Melanoma	NOG	s.c.	26	88.4%	Einarsdottir, 2014 [116]
	NSG	s.c.	694	65.8%	Krepler, 2017 [117]

\* s.c., subcutaneous, \*\* mammarian fat pad, \*\*\* r.c., renal capsule.

The PDX in humanized mice (humanized PDX) has been established for several types of tumors [91,118–120]. The humanized PDX mice model offers a unique platform for examining human acquired and innate immune responses to clinically-relevant tumors and for evaluating immune therapy [121]. However, current models of humanized PDX mice still have several limitations: 1) the balance of hematopoietic and immune cells remains different from that in humans; 2) since the source of HSC is not the same as that of the tumor, it is challenging to match the HLA. These issues require attention for the development of a patient-similar immune response PDX model.

A specific population of immune cells can be reconstituted in highly immunocompromised mice. Human mature T lymphocytes can reconstitute in the classical PBMC transplanted model, although

the duration is relatively short (4–8 weeks) and most of the T lymphocytes are activated [11]. We succeeded in reconstituting human B and T cells and immune response by transplantation of PBMCs into the spleens of NOJ mice [122]. Functional human NK cells and  $\gamma\delta$ T cells can be reconstituted in severe immunocompromised mice and have been used to evaluate the anti-tumor effects of these cells [123,124]. These systems can be applied for the evaluation of cancer immunotherapies such as adoptive cell therapy (NK, gamma delta T ( $\gamma\delta$ T), NK T (NKT), chimeric antigen receptor T (CAR T) cell therapies), antibody therapy (direct killing activity, antibody-dependent cellular cytotoxicity (ADCC), antibody-dependent cellular phagocytosis (ADCP), and complement-dependent cytotoxicity (CDC)), and immune check point blockade therapy.

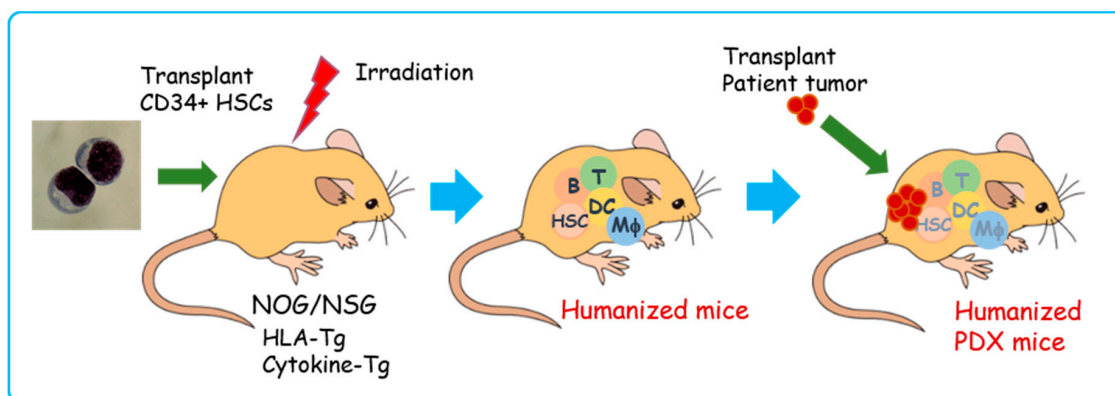


**Figure 6.** Schematic illustration of humanized PDX model generation. First, CD34+ human hematopoietic stem cells are transplanted into irradiated human leukocyte antigen (HLA)/human cytokine transgenic (Tg) NOG/NSG mice. Then, human hematopoietic and immune systems are reconstituted within 8–12 weeks (humanized mice). Patient-derived tumors are transplanted into humanized mice (humanized PDX mice). T: T lymphocytes, B: B lymphocytes, DCs: dendritic cells, M $\phi$ : macrophages, HSCs: hematopoietic stem cells, HLA-Tg: human leukocyte antigen class I and II transgenic mice, Cytokine-Tg: human cytokine (stem cell factor (SCF), IL-3, granulocyte-monocyte colony stimulating factor (GM-CSF), thrombopoietin (TPO), etc.) transgenic mice.

## 7. Perspective

Developments in xenograft technology and highly immunocompromised mice such as NOG/NSG allow us to broaden the application of the PDX platform. Nevertheless, PDX models still require optimization for clinical relevance. The human stromal components are rapidly lost and replaced by the murine microenvironment during engraftment [125]. Recently, it was reported that PDX models undergo mouse-specific tumor evolution with rapid accumulation of copy number alterations during PDX passaging that differed from those acquired during tumor evolution in patients by the strong selection pressures in the mice [126], and only selected clones remain after passages. Thus, current PDX models are not complete “Avatar” models of human cancer. In spite of these findings, PDX models are still the most relevant *in vivo* cancer model for precision medicine, as they keep consistency with their patients’ primary tumor relative to conventional tumor models, especially drug response profiles [127]. Humanized mice with PDX are expected to offer a novel platform for examining immunotherapy (Figure 6) [121]. Despite several limitations, humanized PDX mice have already provided several benefits in studies of cancer behaviors and the functions of immunocompetent cells in tumor microenvironments [118,119,121]. Several attempts have been made to establish humanized microenvironments and generate more comprehensive and functional immune systems in immunocompromised mice [83]. Further development and improvement of these systems will provide an unprecedented platform for personalized cancer medicine, particularly cancer immunotherapy.

The PDX mice models have emerged as important tools for cancer research, with the potential to allow a personalized approach using gene expression and drug sensitivity profiles. However, they have

several limitations that should be noted. Establishment of PDX is time consuming (6 months to 2 years), the success rate varies (10–90%), and it is difficult to retrieve complete patient data. Therefore, many institutions and organizations are focused on creating a large stock of PDX or PDX libraries. European institutions established EurOPDX, a consortium to store PDX, and have already accumulated more than 1500 samples in a PDX bank [128,129]. Jackson Laboratory provides more than 450 samples for researchers [60]. Mega-pharmacies are also establishing their own PDX libraries, and Novartis recently published data on drug screening using 1000 PDX [55]. These PDX biobanks are excellent in vivo platforms for precision medicine [31]. The PDX biobanks with patients' clinical data, pathologies, gene profiles, and drug response data (Figure 4) are critically important for drug response prediction and validation to generate drug response information for tumors from similar genetic backgrounds. Currently, PDX resources are available in the USA and Europe, and most PDX are derived from common cancers. This might create a bias of information. Hence, PDX biobanks in Asia and rare cancer PDX are essential, as is the requirement for a sharing system among PDX biobanks around the world.

**Author Contributions:** Conceptualization, S.O. and K.V.; methodology, R.K.; writing—original draft preparation, S.O.; writing—review and editing, S.O. and K.V.; visualization, S.O.; funding acquisition, S.O. and K.V.

**Funding:** This research was funded by a Grant-in-Aid for Scientific Research from the Ministry of Education, Culture and Sport Science and Technology (MEXT) of Japan (grant number 16K08742); the National Science and Technology Development Agency and the e-Asia Joint Research Program (grant number P1950436, 19jm0210062h0002).

**Acknowledgments:** We thank S. Fujikawa for her technical assistance and Y. Kanagawa for her secretarial work.

**Conflicts of Interest:** The authors declare no conflict of interest.

## References

1. Alteri, E.; Guizzaro, L. Be open about drug failures to speed up research. *Nature* **2018**, *563*, 317–319. [[CrossRef](#)] [[PubMed](#)]
2. DiMasi, J.A.; Reichert, J.M.; Feldman, L.; Malins, A. Clinical approval success rates for investigational cancer drugs. *Clin. Pharmacol. Ther.* **2013**, *94*, 329–335. [[CrossRef](#)] [[PubMed](#)]
3. Ledford, H. Us cancer institute overhauls cell lines. Veteran cells to be replaced by human tumours grown in mice. *Nature* **2016**, *530*, 391. [[CrossRef](#)] [[PubMed](#)]
4. Mestas, J.; Hughes, C.C. Of mice and not men: Differences between mouse and human immunology. *J. Immunol.* **2004**, *172*, 2731–2738. [[CrossRef](#)] [[PubMed](#)]
5. Kojima, Y.; Hayakawa, F.; Morishita, T.; Sugimoto, K.; Minamikawa, Y.; Iwase, M.; Yamamoto, H.; Hirano, D.; Imoto, N.; Shimada, K.; et al. Ym155 induces apoptosis through proteasome-dependent degradation of mcl-1 in primary effusion lymphoma. *Pharmacol. Res.* **2017**, *120*, 242–251. [[CrossRef](#)] [[PubMed](#)]
6. Flanagan, S.P. 'Nude', a new hairless gene with pleiotropic effects in the mouse. *Genet Res.* **1966**, *8*, 295–309. [[CrossRef](#)] [[PubMed](#)]
7. Budzynski, W.; Radzikowski, C. Cytotoxic cells in immunodeficient athymic mice. *Immunopharmacol. Immunotoxicol.* **1994**, *16*, 319–346. [[CrossRef](#)] [[PubMed](#)]
8. Giovanella, B.C.; Fogh, J. The nude mouse in cancer research. *Adv. Cancer Res.* **1985**, *44*, 69–120.
9. Bosma, G.C.; Custer, R.P.; Bosma, M.J. A severe combined immunodeficiency mutation in the mouse. *Nature* **1983**, *301*, 527–530. [[CrossRef](#)]
10. McCune, J.M.; Namikawa, R.; Kaneshima, H.; Shultz, L.D.; Lieberman, M.; Weissman, I.L. The scid-hu mouse: Murine model for the analysis of human hematolymphoid differentiation and function. *Science* **1988**, *241*, 1632–1639. [[CrossRef](#)]
11. Mosier, D.E.; Gulizia, R.J.; Baird, S.M.; Wilson, D.B. Transfer of a functional human immune system to mice with severe combined immunodeficiency. *Nature* **1988**, *335*, 256–259. [[CrossRef](#)] [[PubMed](#)]
12. Taghian, A.; Budach, W.; Zietman, A.; Freeman, J.; Gioioso, D.; Ruka, W.; Suit, H.D. Quantitative comparison between the transplantability of human and murine tumors into the subcutaneous tissue of ncr/sed-nu/nu nude and severe combined immunodeficient mice. *Cancer Res.* **1993**, *53*, 5012–5017. [[PubMed](#)]
13. Roder, J.; Duwe, A. The beige mutation in the mouse selectively impairs natural killer cell function. *Nature* **1979**, *278*, 451–453. [[CrossRef](#)] [[PubMed](#)]

14. Mosier, D.E.; Stell, K.L.; Gulizia, R.J.; Torbett, B.E.; Gilmore, G.L. Homozygous scid/scid; beige/beige mice have low levels of spontaneous or neonatal t cell-induced b cell generation. *J. Exp. Med.* **1993**, *177*, 191–194. [[CrossRef](#)] [[PubMed](#)]
15. Thomsen, M.; Galvani, S.; Canivet, C.; Kamar, N.; Bohler, T. Reconstitution of immunodeficient scid/beige mice with human cells: Applications in preclinical studies. *Toxicology* **2008**, *246*, 18–23. [[CrossRef](#)] [[PubMed](#)]
16. Makino, S.; Kunimoto, K.; Muraoka, Y.; Mizushima, Y.; Katagiri, K.; Tochino, Y. Breeding of a non-obese, diabetic strain of mice. *Jikken Dobutsu. Exp. Anim.* **1980**, *29*, 1–13.
17. Kikutani, H.; Makino, S. The murine autoimmune diabetes model: Nod and related strains. *Adv. Immunol.* **1992**, *51*, 285–322.
18. Shultz, L.D.; Schweitzer, P.A.; Christianson, S.W.; Gott, B.; Schweitzer, I.B.; Tennent, B.; McKenna, S.; Mobraaten, L.; Rajan, T.V.; Greiner, D.L.; et al. Multiple defects in innate and adaptive immunologic function in nod/ltsz-scid mice. *J. Immunol.* **1995**, *154*, 180–191.
19. Notarangelo, L.D.; Giliani, S.; Mazza, C.; Mella, P.; Savoldi, G.; Rodriguez-Perez, C.; Mazzolari, E.; Fiorini, M.; Duse, M.; Plebani, A.; et al. Of genes and phenotypes: The immunological and molecular spectrum of combined immune deficiency. Defects of the gamma(c)-jak3 signaling pathway as a model. *Immunol. Rev.* **2000**, *178*, 39–48. [[CrossRef](#)]
20. Suzuki, K.; Nakajima, H.; Saito, Y.; Saito, T.; Leonard, W.J.; Iwamoto, I. Janus kinase 3 (jak3) is essential for common cytokine receptor gamma chain (gamma(c))-dependent signaling: Comparative analysis of gamma(c), jak3, and gamma(c) and jak3 double-deficient mice. *Int. Immunol.* **2000**, *12*, 123–132. [[CrossRef](#)]
21. Ito, M.; Hiramatsu, H.; Kobayashi, K.; Suzue, K.; Kawahata, M.; Hioki, K.; Ueyama, Y.; Koyanagi, Y.; Sugamura, K.; Tsuji, K.; et al. Nod/scid/gamma(c)(null) mouse: An excellent recipient mouse model for engraftment of human cells. *Blood* **2002**, *100*, 3175–3182. [[CrossRef](#)] [[PubMed](#)]
22. Shultz, L.D.; Lyons, B.L.; Burzenski, L.M.; Gott, B.; Chen, X.; Chaleff, S.; Kotb, M.; Gillies, S.D.; King, M.; Mangada, J.; et al. Human lymphoid and myeloid cell development in nod/ltsz-scid il2r gamma null mice engrafted with mobilized human hemopoietic stem cells. *J. Immunol.* **2005**, *174*, 6477–6489. [[CrossRef](#)] [[PubMed](#)]
23. Okada, S.; Harada, H.; Ito, T.; Saito, T.; Suzu, S. Early development of human hematopoietic and acquired immune systems in new born nod/scid/jak3null mice intrahepatic engrafted with cord blood-derived cd34 + cells. *Int. J. Hematol.* **2008**, *88*, 476–482. [[CrossRef](#)] [[PubMed](#)]
24. McDermott, S.P.; Eppert, K.; Lechman, E.R.; Doedens, M.; Dick, J.E. Comparison of human cord blood engraftment between immunocompromised mouse strains. *Blood* **2010**, *116*, 193–200. [[CrossRef](#)] [[PubMed](#)]
25. Nagatani, M.; Kodera, T.; Suzuki, D.; Igura, S.; Fukunaga, Y.; Kanemitsu, H.; Nakamura, D.; Mochizuki, M.; Kemi, M.; Tamura, K.; et al. Comparison of biological features between severely immuno-deficient nod/shi-scid il2rg(null) and nod/ltsz-scid il2rg(null) mice. *Exp. Anim.* **2019**. [[CrossRef](#)]
26. Navarro-Alvarez, N.; Yang, Y.G. Cd47: A new player in phagocytosis and xenograft rejection. *Cell. Mol. Immunol.* **2011**, *8*, 285–288. [[CrossRef](#)]
27. Takenaka, K.; Prasolava, T.K.; Wang, J.C.; Mortin-Toth, S.M.; Khalouei, S.; Gan, O.I.; Dick, J.E.; Danska, J.S. Polymorphism in sirpa modulates engraftment of human hematopoietic stem cells. *Nat. Immunol.* **2007**, *8*, 1313–1323. [[CrossRef](#)]
28. Yamauchi, T.; Takenaka, K.; Urata, S.; Shima, T.; Kikushige, Y.; Tokuyama, T.; Iwamoto, C.; Nishihara, M.; Iwasaki, H.; Miyamoto, T.; et al. Polymorphic sirpa is the genetic determinant for nod-based mouse lines to achieve efficient human cell engraftment. *Blood* **2013**, *121*, 1316–1325. [[CrossRef](#)]
29. Traggiai, E.; Chicha, L.; Mazzucchelli, L.; Bronz, L.; Piffaretti, J.C.; Lanzavecchia, A.; Manz, M.G. Development of a human adaptive immune system in cord blood cell-transplanted mice. *Science* **2004**, *304*, 104–107. [[CrossRef](#)]
30. Ono, A.; Hattori, S.; Kariya, R.; Iwanaga, S.; Taura, M.; Harada, H.; Suzu, S.; Okada, S. Comparative study of human hematopoietic cell engraftment into balb/c and c57bl/6 strain of rag-2/jak3 double-deficient mice. *J. Biomed Biotechnol.* **2011**, *2011*, 539748. [[CrossRef](#)]
31. Okada, S.; Vaeteewoottacharn, K.; Kariya, R. Establishment of a patient-derived tumor xenograft model and application for precision cancer medicine. *Chem. Pharm. Bull.* **2018**, *66*, 225–230. [[CrossRef](#)] [[PubMed](#)]
32. Iwamoto, C.; Takenaka, K.; Urata, S.; Yamauchi, T.; Shima, T.; Kuriyama, T.; Daitoku, S.; Saito, Y.; Miyamoto, T.; Iwasaki, H.; et al. The balb/c-specific polymorphic sirpa enhances its affinity for human cd47, inhibiting phagocytosis against human cells to promote xenogeneic engraftment. *Exp. Hematol.* **2014**, *42*, 163–171. [[CrossRef](#)] [[PubMed](#)]

33. Goto, H.; Kariya, R.; Matsuda, K.; Kudo, E.; Katano, H.; Okada, S. A potential role of the nod genetic background in mouse peritoneal macrophages for the development of primary effusion lymphoma. *Leuk Res.* **2016**, *42*, 37–42. [[CrossRef](#)] [[PubMed](#)]
34. Goto, H.; Kojima, Y.; Matsuda, K.; Kariya, R.; Taura, M.; Kuwahara, K.; Nagai, H.; Katano, H.; Okada, S. Efficacy of anti-cd47 antibody-mediated phagocytosis with macrophages against primary effusion lymphoma. *Eur. J. Cancer* **2014**, *50*, 1836–1846. [[CrossRef](#)] [[PubMed](#)]
35. Strowig, T.; Rongvaux, A.; Rathinam, C.; Takizawa, H.; Borsotti, C.; Philbrick, W.; Eynon, E.E.; Manz, M.G.; Flavell, R.A. Transgenic expression of human signal regulatory protein alpha in rag2<sup>-/-</sup>gamma(c)<sup>-/-</sup> mice improves engraftment of human hematopoietic cells in humanized mice. *Proc. Natl. Acad. Sci. USA* **2011**, *108*, 13218–13223. [[CrossRef](#)] [[PubMed](#)]
36. Kariya, R.; Matsuda, K.; Gotoh, K.; Vaeteewoottacharn, K.; Hattori, S.; Okada, S. Establishment of nude mice with complete loss of lymphocytes and nk cells and application for in vivo bio-imaging. *Vivo* **2014**, *28*, 779–784.
37. Tanaka, A.; Takeda, S.; Kariya, R.; Matsuda, K.; Urano, E.; Okada, S.; Komano, J. A novel therapeutic molecule against htlv-1 infection targeting provirus. *Leukemia* **2013**, *27*, 1621–1627. [[CrossRef](#)] [[PubMed](#)]
38. Benavides, F.; Oberyszyn, T.M.; VanBuskirk, A.M.; Reeve, V.E.; Kusewitt, D.F. The hairless mouse in skin research. *J. Dermatol. Sci.* **2009**, *53*, 10–18. [[CrossRef](#)] [[PubMed](#)]
39. Heiniger, H.J.; Meier, H.; Kaliss, N.; Cherry, M.; Chen, H.W.; Stoner, R.D. Hereditary immunodeficiency and leukemogenesis in hrs-j mice. *Cancer Res.* **1974**, *34*, 201–211. [[PubMed](#)]
40. Crottes, D.; Rapetti-Mauss, R.; Alcaraz-Perez, F.; Tichet, M.; Gariano, G.; Martial, S.; Guizouarn, H.; Pellissier, B.; Loubat, A.; Popa, A.; et al. Sigmar1 regulates membrane electrical activity in response to extracellular matrix stimulation to drive cancer cell invasiveness. *Cancer Res.* **2016**, *76*, 607–618. [[CrossRef](#)]
41. Smee, D.F.; Dagley, A.; Downs, B.; Hagloch, J.; Tarbet, E.B. Enhanced efficacy of cidofovir combined with vaccinia immune globulin in treating progressive cutaneous vaccinia virus infections in immunosuppressed hairless mice. *Antimicrob. Agents Chemother.* **2015**, *59*, 520–526. [[CrossRef](#)] [[PubMed](#)]
42. Lai, Y.; Wei, X.; Lin, S.; Qin, L.; Cheng, L.; Li, P. Current status and perspectives of patient-derived xenograft models in cancer research. *J. Hematol. Oncol.* **2017**, *10*, 106. [[CrossRef](#)]
43. Hoffman, R. Green fluorescent protein imaging of tumour growth, metastasis, and angiogenesis in mouse models. *Lancet. Oncol.* **2002**, *3*, 546–556. [[CrossRef](#)]
44. Yang, M.; Reynoso, J.; Jiang, P.; Li, L.; Moossa, A.R.; Hoffman, R.M. Transgenic nude mouse with ubiquitous green fluorescent protein expression as a host for human tumors. *Cancer Res.* **2004**, *64*, 8651–8656. [[CrossRef](#)]
45. Niclou, S.P.; Danzeisen, C.; Eikesdal, H.P.; Wiig, H.; Brons, N.H.; Poli, A.M.; Svendsen, A.; Torsvik, A.; Enger, P.O.; Terzis, J.A.; et al. A novel egfp-expressing immunodeficient mouse model to study tumor-host interactions. *FASEB J.* **2008**, *22*, 3120–3128. [[CrossRef](#)] [[PubMed](#)]
46. Gotoh, K.; Kariya, R.; Matsuda, K.; Hattori, S.; Vaeteewoottacharn, K.; Okada, S. A novel egfp-expressing nude mice with complete loss of lymphocytes and nk cells to study tumor-host interactions. *Biosci. Trends* **2014**, *8*, 202–205. [[CrossRef](#)]
47. Hoffman, R.M.; Bouvet, M. Imaging the microenvironment of pancreatic cancer patient-derived orthotopic xenografts (pdox) growing in transgenic nude mice expressing gfp, rfp, or cfp. *Cancer Lett.* **2016**, *380*, 349–355. [[CrossRef](#)]
48. Vaeteewoottacharn, K.; Kariya, R.; Dana, P.; Fujikawa, S.; Matsuda, K.; Ohkuma, K.; Kudo, E.; Kraiklang, R.; Wongkham, C.; Wongkham, S.; et al. Inhibition of carbonic anhydrase potentiates bevacizumab treatment in cholangiocarcinoma. *Tumour Biol. J. Int. Soc. Oncodevelopmental Biol. Med.* **2016**, *37*, 9023–9035. [[CrossRef](#)]
49. Tentler, J.J.; Tan, A.C.; Weekes, C.D.; Jimeno, A.; Leong, S.; Pitts, T.M.; Arcaroli, J.J.; Messersmith, W.A.; Eckhardt, S.G. Patient-derived tumour xenografts as models for oncology drug development. *Nat. Rev. Clin. Oncol.* **2012**, *9*, 338–350. [[CrossRef](#)]
50. Cassidy, J.W.; Caldas, C.; Bruna, A. Maintaining tumor heterogeneity in patient-derived tumor xenografts. *Cancer Res.* **2015**, *75*, 2963–2968. [[CrossRef](#)]
51. Wang, D.; Pham, N.A.; Tong, J.; Sakashita, S.; Allo, G.; Kim, L.; Yanagawa, N.; Raghavan, V.; Wei, Y.; To, C.; et al. Molecular heterogeneity of non-small cell lung carcinoma patient-derived xenografts closely reflect their primary tumors. *Int. J. Cancer* **2017**, *140*, 662–673. [[CrossRef](#)] [[PubMed](#)]
52. Gargiulo, G. Next-generation in vivo modeling of human cancers. *Front. Oncol.* **2018**, *8*, 429. [[CrossRef](#)]



53. Collins, A.T.; Lang, S.H. A systematic review of the validity of patient derived xenograft (pdx) models: The implications for translational research and personalised medicine. *PeerJ* **2018**, *6*, e5981. [[CrossRef](#)]
54. Bleijs, M.; van de Wetering, M.; Clevers, H.; Drost, J. Xenograft and organoid model systems in cancer research. *EMBO J.* **2019**, *38*, e101654. [[CrossRef](#)]
55. Gao, H.; Korn, J.M.; Ferretti, S.; Monahan, J.E.; Wang, Y.; Singh, M.; Zhang, C.; Schnell, C.; Yang, G.; Zhang, Y.; et al. High-throughput screening using patient-derived tumor xenografts to predict clinical trial drug response. *Nat. Med.* **2015**, *21*, 1318–1325. [[CrossRef](#)] [[PubMed](#)]
56. Pompili, L.; Porru, M.; Caruso, C.; Biroccio, A.; Leonetti, C. Patient-derived xenografts: A relevant preclinical model for drug development. *J. Exp. Clin. Cancer Res. Cr* **2016**, *35*, 189. [[CrossRef](#)]
57. Vaeteewoottacharn, K.; Pairojkul, C.; Kariya, R.; Muisuk, K.; Imtawil, K.; Chamgramol, Y.; Bhudhisawasdi, V.; Khuntikeo, N.; Pugkhem, A.; Saeseow, O.T.; et al. Establishment of highly transplantable cholangiocarcinoma cell lines from a patient-derived xenograft mouse model. *Cells* **2019**, *8*. [[CrossRef](#)] [[PubMed](#)]
58. Jin, K.; Teng, L.; Shen, Y.; He, K.; Xu, Z.; Li, G. Patient-derived human tumour tissue xenografts in immunodeficient mice: A systematic review. *Clin. Transl. Oncol.* **2010**, *12*, 473–480. [[CrossRef](#)] [[PubMed](#)]
59. Chijiwa, T.; Kawai, K.; Noguchi, A.; Sato, H.; Hayashi, A.; Cho, H.; Shiozawa, M.; Kishida, T.; Morinaga, S.; Yokose, T.; et al. Establishment of patient-derived cancer xenografts in immunodeficient nog mice. *Int. J. Oncol.* **2015**, *47*, 61–70. [[CrossRef](#)]
60. Shultz, L.D.; Goodwin, N.; Ishikawa, F.; Hosur, V.; Lyons, B.L.; Greiner, D.L. Human cancer growth and therapy in immunodeficient mouse models. *Cold Spring Harb. Protoc.* **2014**, *2014*, 694–708. [[CrossRef](#)] [[PubMed](#)]
61. Brown, K.M.; Xue, A.; Mittal, A.; Samra, J.S.; Smith, R.; Hugh, T.J. Patient-derived xenograft models of colorectal cancer in pre-clinical research: A systematic review. *Oncotarget* **2016**, *7*, 66212–66225. [[CrossRef](#)] [[PubMed](#)]
62. Xu, C.; Li, X.; Liu, P.; Li, M.; Luo, F. Patient-derived xenograft mouse models: A high fidelity tool for individualized medicine. *Oncol. Lett.* **2019**, *17*, 3–10. [[CrossRef](#)] [[PubMed](#)]
63. Sittithumcharee, G.; Suppramote, O.; Vaeteewoottacharn, K.; Sirisuksakun, C.; Jamnongsong, S.; Lapanuwat, P.; Suntiparpluacha, M.; Matha, A.; Chusorn, P.; Buraphat, P.; et al. Dependency of cholangiocarcinoma on cyclin d-dependent kinase activity. *Hepatology* **2019**. [[CrossRef](#)] [[PubMed](#)]
64. Murayama, T.; Gotoh, N. Patient-derived xenograft models of breast cancer and their application. *Cells* **2019**, *8*. [[CrossRef](#)] [[PubMed](#)]
65. Hoffman, R.M. Patient-derived orthotopic xenografts: Better mimic of metastasis than subcutaneous xenografts. *Nat. Rev. Cancer* **2015**, *15*, 451–452. [[CrossRef](#)] [[PubMed](#)]
66. Wang, Y.; Revelo, M.P.; Sudilovsky, D.; Cao, M.; Chen, W.G.; Goetz, L.; Xue, H.; Sadar, M.; Shappell, S.B.; Cunha, G.R.; et al. Development and characterization of efficient xenograft models for benign and malignant human prostate tissue. *Prostate* **2005**, *64*, 149–159. [[CrossRef](#)]
67. Cho, S.Y.; Kang, W.; Han, J.Y.; Min, S.; Kang, J.; Lee, A.; Kwon, J.Y.; Lee, C.; Park, H. An integrative approach to precision cancer medicine using patient-derived xenografts. *Mol. Cells* **2016**, *39*, 77–86.
68. Whittle, J.R.; Lewis, M.T.; Lindeman, G.J.; Visvader, J.E. Patient-derived xenograft models of breast cancer and their predictive power. *Breast Cancer Res. Bcr* **2015**, *17*, 17. [[CrossRef](#)]
69. Centenera, M.M.; Hickey, T.E.; Jindal, S.; Ryan, N.K.; Ravindranathan, P.; Mohammed, H.; Robinson, J.L.; Schiewer, M.J.; Ma, S.; Kapur, P.; et al. A patient-derived explant (pde) model of hormone-dependent cancer. *Mol. Oncol.* **2018**, *12*, 1608–1622. [[CrossRef](#)]
70. Oyama, R.; Takahashi, M.; Yoshida, A.; Sakumoto, M.; Takai, Y.; Kito, F.; Shiozawa, K.; Qiao, Z.; Arai, Y.; Shibata, T.; et al. Generation of novel patient-derived cix-dux4 sarcoma xenografts and cell lines. *Sci. Rep.* **2017**, *7*, 4712. [[CrossRef](#)]
71. Borodovsky, A.; McQuiston, T.J.; Stetson, D.; Ahmed, A.; Whitston, D.; Zhang, J.; Grondine, M.; Lawson, D.; Challberg, S.S.; Zinda, M.; et al. Generation of stable pdx derived cell lines using conditional reprogramming. *Mol. Cancer* **2017**, *16*, 177. [[CrossRef](#)] [[PubMed](#)]
72. Shima, K.; Mizuma, M.; Hayashi, H.; Nakagawa, K.; Okada, T.; Sakata, N.; Omura, N.; Kitamura, Y.; Motoi, F.; Rikiyama, T.; et al. Potential utility of egfp-expressing nog mice (nog-egfp) as a high purity cancer sampling system. *J. Exp. Clin. Cancer Res. Cr* **2012**, *31*, 55. [[CrossRef](#)] [[PubMed](#)]
73. Waldmann, T.A. Immunotherapy: Past, present and future. *Nat. Med.* **2003**, *9*, 269–277. [[CrossRef](#)] [[PubMed](#)]
74. Pardoll, D.M. The blockade of immune checkpoints in cancer immunotherapy. *Nat. Rev. Cancer* **2012**, *12*, 252–264. [[CrossRef](#)] [[PubMed](#)]

75. Zhang, H.; Chen, J. Current status and future directions of cancer immunotherapy. *J. Cancer* **2018**, *9*, 1773–1781. [[CrossRef](#)] [[PubMed](#)]
76. Shultz, L.D.; Ishikawa, F.; Greiner, D.L. Humanized mice in translational biomedical research. *Nat. Rev. Immunol.* **2007**, *7*, 118–130. [[CrossRef](#)] [[PubMed](#)]
77. Lan, P.; Tonomura, N.; Shimizu, A.; Wang, S.; Yang, Y.G. Reconstitution of a functional human immune system in immunodeficient mice through combined human fetal thymus/liver and cd34+ cell transplantation. *Blood* **2006**, *108*, 487–492. [[CrossRef](#)] [[PubMed](#)]
78. Morton, J.J.; Bird, G.; Refaeli, Y.; Jimeno, A. Humanized mouse xenograft models: Narrowing the tumor-microenvironment gap. *Cancer Res.* **2016**, *76*, 6153–6158. [[CrossRef](#)] [[PubMed](#)]
79. De La Rochere, P.; Guil-Luna, S.; Decaudin, D.; Azar, G.; Sidhu, S.S.; Piaggio, E. Humanized mice for the study of immuno-oncology. *Trends Immunol.* **2018**, *39*, 748–763. [[CrossRef](#)] [[PubMed](#)]
80. Billerbeck, E.; Barry, W.T.; Mu, K.; Dorner, M.; Rice, C.M.; Ploss, A. Development of human cd4+foxp3+ regulatory t cells in human stem cell factor-, granulocyte-macrophage colony-stimulating factor-, and interleukin-3-expressing nod-scid il2rgamma(null) humanized mice. *Blood* **2011**, *117*, 3076–3086. [[CrossRef](#)]
81. Shultz, L.D.; Saito, Y.; Najima, Y.; Tanaka, S.; Ochi, T.; Tomizawa, M.; Doi, T.; Sone, A.; Suzuki, N.; Fujiwara, H.; et al. Generation of functional human t-cell subsets with hla-restricted immune responses in hla class i expressing nod/scid/il2r gamma(null) humanized mice. *Proc. Natl. Acad. Sci. USA* **2010**, *107*, 13022–13027. [[CrossRef](#)] [[PubMed](#)]
82. Zeng, Y.; Liu, B.; Rubio, M.T.; Wang, X.; Ojcius, D.M.; Tang, R.; Durrbach, A.; Ru, Z.; Zhou, Y.; Lone, Y.C. Creation of an immunodeficient hla-transgenic mouse (humamice) and functional validation of human immunity after transfer of hla-matched human cells. *PLoS ONE* **2017**, *12*, e0173754. [[CrossRef](#)] [[PubMed](#)]
83. Theocharides, A.P.; Rongvaux, A.; Fritsch, K.; Flavell, R.A.; Manz, M.G. Humanized hemato-lymphoid system mice. *Haematologica* **2016**, *101*, 5–19. [[CrossRef](#)] [[PubMed](#)]
84. Ojima, H.; Yoshikawa, D.; Ino, Y.; Shimizu, H.; Miyamoto, M.; Kokubu, A.; Hiraoka, N.; Morofuji, N.; Kondo, T.; Onaya, H.; et al. Establishment of six new human biliary tract carcinoma cell lines and identification of mageh1 as a candidate biomarker for predicting the efficacy of gemcitabine treatment. *Cancer Sci.* **2010**, *101*, 882–888. [[CrossRef](#)] [[PubMed](#)]
85. Cavalloni, G.; Peraldo-Neia, C.; Sassi, F.; Chiorino, G.; Sarotto, I.; Aglietta, M.; Leone, F. Establishment of a patient-derived intrahepatic cholangiocarcinoma xenograft model with kras mutation. *BMC Cancer* **2016**, *16*, 90. [[CrossRef](#)] [[PubMed](#)]
86. Julien, S.; Merino-Trigo, A.; Lacroix, L.; Pocard, M.; Goere, D.; Mariani, P.; Landron, S.; Bigot, L.; Nemati, F.; Dartigues, P.; et al. Characterization of a large panel of patient-derived tumor xenografts representing the clinical heterogeneity of human colorectal cancer. *Clin. Cancer Res.* **2012**, *18*, 5314–5328. [[CrossRef](#)] [[PubMed](#)]
87. Bertotti, A.; Migliardi, G.; Galimi, F.; Sassi, F.; Torti, D.; Isella, C.; Cora, D.; Di Nicolantonio, F.; Buscarino, M.; Petti, C.; et al. A molecularly annotated platform of patient-derived xenografts (“xenopatients”) identifies her2 as an effective therapeutic target in cetuximab-resistant colorectal cancer. *Cancer Discov.* **2011**, *1*, 508–523. [[CrossRef](#)] [[PubMed](#)]
88. Chou, J.; Fitzgibbon, M.P.; Mortales, C.L.; Towler, A.M.; Upton, M.P.; Yeung, R.S.; McIntosh, M.W.; Warren, E.H. Phenotypic and transcriptional fidelity of patient-derived colon cancer xenografts in immune-deficient mice. *PLoS ONE* **2013**, *8*, e79874. [[CrossRef](#)]
89. Garrido-Laguna, I.; Uson, M.; Rajeshkumar, N.V.; Tan, A.C.; de Oliveira, E.; Karikari, C.; Villaroel, M.C.; Salomon, A.; Taylor, G.; Sharma, R.; et al. Tumor engraftment in nude mice and enrichment in stroma-related gene pathways predict poor survival and resistance to gemcitabine in patients with pancreatic cancer. *Clin. Cancer Res.* **2011**, *17*, 5793–5800. [[CrossRef](#)]
90. Mattie, M.; Christensen, A.; Chang, M.S.; Yeh, W.; Said, S.; Shostak, Y.; Capo, L.; Verlinsky, A.; An, Z.; Joseph, I.; et al. Molecular characterization of patient-derived human pancreatic tumor xenograft models for preclinical and translational development of cancer therapeutics. *Neoplasia* **2013**, *15*, 1138–1150. [[CrossRef](#)]
91. Guo, S.; Gao, S.; Liu, R.; Shen, J.; Shi, X.; Bai, S.; Wang, H.; Zheng, K.; Shao, Z.; Liang, C.; et al. Oncological and genetic factors impacting pdx model construction with nsg mice in pancreatic cancer. *FASEB J.* **2019**, *33*, 873–884. [[CrossRef](#)] [[PubMed](#)]
92. Wang, H.; Lu, J.; Tang, J.; Chen, S.; He, K.; Jiang, X.; Jiang, W.; Teng, L. Establishment of patient-derived gastric cancer xenografts: A useful tool for preclinical evaluation of targeted therapies involving alterations in her-2, met and fgfr2 signaling pathways. *BMC Cancer* **2017**, *17*, 191. [[CrossRef](#)] [[PubMed](#)]

93. Zhu, Y.; Tian, T.; Li, Z.; Tang, Z.; Wang, L.; Wu, J.; Li, Y.; Dong, B.; Li, N.; Zou, J.; et al. Establishment and characterization of patient-derived tumor xenograft using gastroscopic biopsies in gastric cancer. *Sci. Rep.* **2015**, *5*, 8542. [[CrossRef](#)] [[PubMed](#)]
94. Zhang, T.; Zhang, L.; Fan, S.; Zhang, M.; Fu, H.; Liu, Y.; Yin, X.; Chen, H.; Xie, L.; Zhang, J.; et al. Patient-derived gastric carcinoma xenograft mouse models faithfully represent human tumor molecular diversity. *PLoS ONE* **2015**, *10*, e0134493. [[CrossRef](#)] [[PubMed](#)]
95. Choi, Y.Y.; Lee, J.E.; Kim, H.; Sim, M.H.; Kim, K.K.; Lee, G.; Kim, H.I.; An, J.Y.; Hyung, W.J.; Kim, C.B.; et al. Establishment and characterisation of patient-derived xenografts as preclinical models for gastric cancer. *Sci. Rep.* **2016**, *6*, 22172. [[CrossRef](#)] [[PubMed](#)]
96. Keysar, S.B.; Astling, D.P.; Anderson, R.T.; Vogler, B.W.; Bowles, D.W.; Morton, J.J.; Paylor, J.J.; Glogowska, M.J.; Le, P.N.; Eagles-Soukup, J.R.; et al. A patient tumor transplant model of squamous cell cancer identifies pi3k inhibitors as candidate therapeutics in defined molecular bins. *Mol. Oncol.* **2013**, *7*, 776–790. [[CrossRef](#)] [[PubMed](#)]
97. Kimple, R.J.; Harari, P.M.; Torres, A.D.; Yang, R.Z.; Soriano, B.J.; Yu, M.; Armstrong, E.A.; Blitzer, G.C.; Smith, M.A.; Lorenz, L.D.; et al. Development and characterization of hpv-positive and hpv-negative head and neck squamous cell carcinoma tumorgrafts. *Clin. Cancer Res.* **2013**, *19*, 855–864. [[CrossRef](#)] [[PubMed](#)]
98. Marangoni, E.; Vincent-Salomon, A.; Auger, N.; Degeorges, A.; Assayag, F.; de Cremoux, P.; de Plater, L.; Guyader, C.; De Pinieux, G.; Judde, J.G.; et al. A new model of patient tumor-derived breast cancer xenografts for preclinical assays. *Clin. Cancer Res.* **2007**, *13*, 3989–3998. [[CrossRef](#)] [[PubMed](#)]
99. Cottu, P.; Marangoni, E.; Assayag, F.; de Cremoux, P.; Vincent-Salomon, A.; Guyader, C.; de Plater, L.; Elbaz, C.; Karboul, N.; Fontaine, J.J.; et al. Modeling of response to endocrine therapy in a panel of human luminal breast cancer xenografts. *Breast Cancer Res. Treat.* **2012**, *133*, 595–606. [[CrossRef](#)] [[PubMed](#)]
100. DeRose, Y.S.; Wang, G.; Lin, Y.C.; Bernard, P.S.; Buys, S.S.; Ebbert, M.T.; Factor, R.; Matsen, C.; Milash, B.A.; Nelson, E.; et al. Tumor grafts derived from women with breast cancer authentically reflect tumor pathology, growth, metastasis and disease outcomes. *Nat. Med.* **2011**, *17*, 1514–1520. [[CrossRef](#)] [[PubMed](#)]
101. Zhang, X.; Claerhout, S.; Prat, A.; Dobrolecki, L.E.; Petrovic, I.; Lai, Q.; Landis, M.D.; Wiechmann, L.; Schiff, R.; Giuliano, M.; et al. A renewable tissue resource of phenotypically stable, biologically and ethnically diverse, patient-derived human breast cancer xenograft models. *Cancer Res.* **2013**, *73*, 4885–4897. [[CrossRef](#)] [[PubMed](#)]
102. Ricci, F.; Bizzaro, F.; Cesca, M.; Guffanti, F.; Ganzinelli, M.; Decio, A.; Ghilardi, C.; Perego, P.; Fruscio, R.; Buda, A.; et al. Patient-derived ovarian tumor xenografts recapitulate human clinicopathology and genetic alterations. *Cancer Res.* **2014**, *74*, 6980–6990. [[CrossRef](#)] [[PubMed](#)]
103. Heo, E.J.; Cho, Y.J.; Cho, W.C.; Hong, J.E.; Jeon, H.K.; Oh, D.Y.; Choi, Y.L.; Song, S.Y.; Choi, J.J.; Bae, D.S.; et al. Patient-derived xenograft models of epithelial ovarian cancer for preclinical studies. *Cancer Res. Treat.* **2017**, *49*, 915–926. [[CrossRef](#)] [[PubMed](#)]
104. Dobbin, Z.C.; Katre, A.A.; Steg, A.D.; Erickson, B.K.; Shah, M.M.; Alvarez, R.D.; Conner, M.G.; Schneider, D.; Chen, D.; Landen, C.N. Using heterogeneity of the patient-derived xenograft model to identify the chemoresistant population in ovarian cancer. *Oncotarget* **2014**, *5*, 8750–8764. [[CrossRef](#)] [[PubMed](#)]
105. Weroha, S.J.; Becker, M.A.; Enderica-Gonzalez, S.; Harrington, S.C.; Oberg, A.L.; Maurer, M.J.; Perkins, S.E.; AlHilli, M.; Butler, K.A.; McKinstry, S.; et al. Tumorgrafts as in vivo surrogates for women with ovarian cancer. *Clin. Cancer Res.* **2014**, *20*, 1288–1297. [[CrossRef](#)] [[PubMed](#)]
106. Topp, M.D.; Hartley, L.; Cook, M.; Heong, V.; Boehm, E.; McShane, L.; Pyman, J.; McNally, O.; Ananda, S.; Harrell, M.; et al. Molecular correlates of platinum response in human high-grade serous ovarian cancer patient-derived xenografts. *Mol. Oncol.* **2014**, *8*, 656–668. [[CrossRef](#)] [[PubMed](#)]
107. Fichtner, I.; Rolff, J.; Soong, R.; Hoffmann, J.; Hammer, S.; Sommer, A.; Becker, M.; Merk, J. Establishment of patient-derived non-small cell lung cancer xenografts as models for the identification of predictive biomarkers. *Clin. Cancer Res.* **2008**, *14*, 6456–6468. [[CrossRef](#)] [[PubMed](#)]
108. Dong, X.; Guan, J.; English, J.C.; Flint, J.; Yee, J.; Evans, K.; Murray, N.; Macaulay, C.; Ng, R.T.; Gout, P.W.; et al. Patient-derived first generation xenografts of non-small cell lung cancers: Promising tools for predicting drug responses for personalized chemotherapy. *Clin. Cancer Res.* **2010**, *16*, 1442–1451. [[CrossRef](#)] [[PubMed](#)]
109. Chen, Y.; Zhang, R.; Wang, L.; Correa, A.M.; Pataer, A.; Xu, Y.; Zhang, X.; Ren, C.; Wu, S.; Meng, Q.H.; et al. Tumor characteristics associated with engraftment of patient-derived non-small cell lung cancer xenografts in immunocompromised mice. *Cancer* **2019**. [[CrossRef](#)]

110. Brabetz, S.; Leary, S.E.S.; Grobner, S.N.; Nakamoto, M.W.; Seker-Cin, H.; Girard, E.J.; Cole, B.; Strand, A.D.; Bloom, K.L.; Hovestadt, V.; et al. A biobank of patient-derived pediatric brain tumor models. *Nat. Med.* **2018**, *24*, 1752–1761. [[CrossRef](#)]
111. Priolo, C.; Agostini, M.; Vena, N.; Ligon, A.H.; Fiorentino, M.; Shin, E.; Farsetti, A.; Pontecorvi, A.; Sicinska, E.; Loda, M. Establishment and genomic characterization of mouse xenografts of human primary prostate tumors. *Am. J. Pathol.* **2010**, *176*, 1901–1913. [[CrossRef](#)] [[PubMed](#)]
112. Wetterauer, C.; Vlajnic, T.; Schuler, J.; Gsponer, J.R.; Thalmann, G.N.; Cecchini, M.; Schneider, J.; Zellweger, T.; Pueschel, H.; Bachmann, A.; et al. Early development of human lymphomas in a prostate cancer xenograft program using triple knock-out immunocompromised mice. *Prostate* **2015**, *75*, 585–592. [[CrossRef](#)] [[PubMed](#)]
113. Lang, H.; Beraud, C.; Bethry, A.; Danilin, S.; Lindner, V.; Coquard, C.; Rothhut, S.; Massfelder, T. Establishment of a large panel of patient-derived preclinical models of human renal cell carcinoma. *Oncotarget* **2016**, *7*, 59336–59359. [[CrossRef](#)] [[PubMed](#)]
114. Sivanand, S.; Pena-Llopis, S.; Zhao, H.; Kucejova, B.; Spence, P.; Pavia-Jimenez, A.; Yamasaki, T.; McBride, D.J.; Gillen, J.; Wolff, N.C.; et al. A validated tumorgraft model reveals activity of dovitinib against renal cell carcinoma. *Sci. Transl. Med.* **2012**, *4*, 137ra175. [[CrossRef](#)] [[PubMed](#)]
115. Dong, Y.; Manley, B.J.; Becerra, M.F.; Redzematovic, A.; Casuscelli, J.; Tennenbaum, D.M.; Reznik, E.; Han, S.; Benfante, N.; Chen, Y.B.; et al. Tumor xenografts of human clear cell renal cell carcinoma but not corresponding cell lines recapitulate clinical response to sunitinib: Feasibility of using biopsy samples. *Eur. Urol. Focus* **2017**, *3*, 590–598. [[CrossRef](#)] [[PubMed](#)]
116. Einarsdottir, B.O.; Bagge, R.O.; Bhadury, J.; Jespersen, H.; Mattsson, J.; Nilsson, L.M.; Truve, K.; Lopez, M.D.; Naredi, P.; Nilsson, O.; et al. Melanoma patient-derived xenografts accurately model the disease and develop fast enough to guide treatment decisions. *Oncotarget* **2014**, *5*, 9609–9618. [[CrossRef](#)] [[PubMed](#)]
117. Krepler, C.; Sproesser, K.; Brafford, P.; Beqiri, M.; Garman, B.; Xiao, M.; Shannan, B.; Watters, A.; Perego, M.; Zhang, G.; et al. A comprehensive patient-derived xenograft collection representing the heterogeneity of melanoma. *Cell Rep.* **2017**, *21*, 1953–1967. [[CrossRef](#)]
118. Zhao, Y.; Shuen, T.W.H.; Toh, T.B.; Chan, X.Y.; Liu, M.; Tan, S.Y.; Fan, Y.; Yang, H.; Lyer, S.G.; Bonney, G.K.; et al. Development of a new patient-derived xenograft humanised mouse model to study human-specific tumour microenvironment and immunotherapy. *Gut* **2018**, *67*, 1845–1854. [[CrossRef](#)]
119. Yao, L.C.; Aryee, K.E.; Cheng, M.; Kaur, P.; Keck, J.G.; Brehm, M.A. Creation of pdx-bearing humanized mice to study immuno-oncology. *Methods Mol. Biol.* **2019**, *1953*, 241–252.
120. Buque, A.; Galluzzi, L. Modeling tumor immunology and immunotherapy in mice. *Trends Cancer* **2018**, *4*, 599–601. [[CrossRef](#)]
121. Choi, Y.; Lee, S.; Kim, K.; Kim, S.H.; Chung, Y.J.; Lee, C. Studying cancer immunotherapy using patient-derived xenografts (pdxs) in humanized mice. *Exp. Mol. Med.* **2018**, *50*, 99. [[CrossRef](#)] [[PubMed](#)]
122. Satoh, M.; Saito, M.; Tanaka, K.; Iwanaga, S.; Ali, S.N.; Seki, T.; Okada, S.; Kohara, M.; Harada, S.; Kai, C.; et al. Evaluation of a recombinant measles virus expressing hepatitis c virus envelope proteins by infection of human pbl-nod/scid/jak3null mouse. *Comp. Immunol. Microbiol. Infect. Dis.* **2010**, *33*, e81–e88. [[CrossRef](#)] [[PubMed](#)]
123. Harada, H.; Suzu, S.; Ito, T.; Okada, S. Selective expansion and engraftment of human cd16+ nk cells in nod/scid mice. *Eur. J. Immunol.* **2005**, *35*, 3599–3609. [[CrossRef](#)] [[PubMed](#)]
124. Goto, H.; Matsuda, K.; Srikoon, P.; Kariya, R.; Hattori, S.; Taura, M.; Katano, H.; Okada, S. Potent antitumor activity of zoledronic acid-induced vgamma9vdelta2 t cells against primary effusion lymphoma. *Cancer Lett.* **2013**, *331*, 174–182. [[CrossRef](#)] [[PubMed](#)]
125. Liu, Y.; Chanana, P.; Davila, J.I.; Hou, X.; Zanfagnin, V.; McGehee, C.D.; Goode, E.L.; Polley, E.C.; Haluska, P.; Weroha, S.J.; et al. Gene expression differences between matched pairs of ovarian cancer patient tumors and patient-derived xenografts. *Sci. Rep.* **2019**, *9*, 6314. [[CrossRef](#)] [[PubMed](#)]
126. Ben-David, U.; Ha, G.; Tseng, Y.Y.; Greenwald, N.F.; Oh, C.; Shih, J.; McFarland, J.M.; Wong, B.; Boehm, J.S.; Beroukhim, R.; et al. Patient-derived xenografts undergo mouse-specific tumor evolution. *Nat. Genet.* **2017**, *49*, 1567–1575. [[CrossRef](#)] [[PubMed](#)]
127. Aparicio, S.; Hidalgo, M.; Kung, A.L. Examining the utility of patient-derived xenograft mouse models. *Nat. Rev. Cancer* **2015**, *15*, 311–316. [[CrossRef](#)] [[PubMed](#)]

128. Hidalgo, M.; Amant, F.; Biankin, A.V.; Budinska, E.; Byrne, A.T.; Caldas, C.; Clarke, R.B.; de Jong, S.; Jonkers, J.; Maelandsmo, G.M.; et al. Patient-derived xenograft models: An emerging platform for translational cancer research. *Cancer Discov.* **2014**, *4*, 998–1013. [[CrossRef](#)] [[PubMed](#)]
129. Byrne, A.T.; Alferez, D.G.; Amant, F.; Annibaldi, D.; Arribas, J.; Biankin, A.V.; Bruna, A.; Budinska, E.; Caldas, C.; Chang, D.K.; et al. Interrogating open issues in cancer precision medicine with patient-derived xenografts. *Nat. Rev. Cancer* **2017**, *17*, 254–268. [[CrossRef](#)]



© 2019 by the authors. Licensee MDPI, Basel, Switzerland. This article is an open access article distributed under the terms and conditions of the Creative Commons Attribution (CC BY) license (<http://creativecommons.org/licenses/by/4.0/>).